Chemosphere 197 (2018) 611–621

Contents lists available at ScienceDirect

Chemosphere

journal homepage: www.elsevier.com/locate/chemosphere

Developmental toxicity induced by PM2.5 through endoplasmic reticulum stress and autophagy pathway in zebrafish embryos

Yun Zhang [a, *], Saiyu Li [b], Juanjuan Li [a, c], Liwen Han [a], Qiuxia He [a], Rongchun Wang [a], Ximin Wang [a], Kechun Liu [a, **]

[a] Biology Institute, Qilu University of Technology (Shandong Academy of Sciences), Key Laboratory for Drug Screening Technology of Shandong Academy of Sciences, Shandong Provincial Engineering Laboratory for Biological Testing Technology, 28789 Jingshidong Road, Licheng District, Jinan, 250103, Shandong Province, PR China
[b] Shandong Analysis and Test Center, 19 Keyuan Road, Lixia District, Jinan, 250014, Shandong Province, PR China
[c] Shanxi Medical University, 56 Xinjiannan Road, Yingze District, Taiyuan, 030001, Shanxi Province, PR China

HIGHLIGHTS

- $PM_{2.5}$ caused a dose- and time-dependent increase in the developmental toxicity of zebrafish embryos.
- $PM_{2.5}$ reduced the locomotor capacity of zebrafish embryos.
- $PM_{2.5}$ induced inflammation and promoted the ERS and autophagy responses via IRE1-XBP1 and ATF6 pathways.
- ERS and autophagy responses mediated the developmental toxicity induced by $PM_{2.5}$ in zebrafish embryos.

GRAPHICAL ABSTRACT

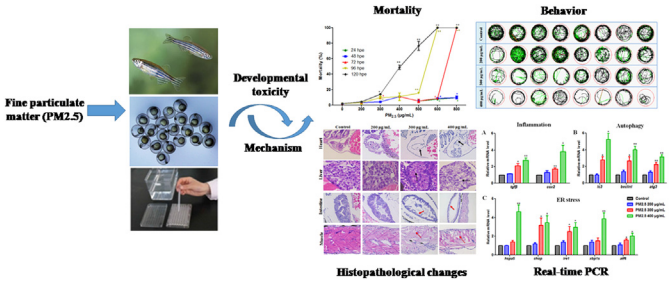

ARTICLE INFO

Article history:
Received 6 November 2017
Received in revised form
19 January 2018
Accepted 21 January 2018
Available online 1 February 2018

Handling Editor: David Volz

Keywords:
$PM_{2.5}$
Zebrafish embryos
Developmental toxicity
Endoplasmic reticulum stress
Autophagy

ABSTRACT

The aims of this study were to investigate the mechanism underlying the developmental toxicity of fine particulate matter ($PM_{2.5}$) and provide a more thorough understanding of the toxicity of $PM_{2.5}$ in an ecological environment. Zebrafish embryos at 4 h post-fertilization were exposed to $PM_{2.5}$ at doses of 200, 300, 400, 500, 600 and 800 μg/mL for 120 h. The mortality, hatching rate, morphology score, body length, locomotor capacity, histological changes, antioxidant defense system, leukocyte migration, inflammation-related gene mRNA expression, endoplasmic reticulum stress (ERS) and autophagy were evaluated to study $PM_{2.5}$-induced developmental toxicity and its underlying mechanisms. $PM_{2.5}$ exposure significantly increased the mortality and malformations and reduced the hatching rate and body length of the zebrafish. $PM_{2.5}$ significantly reduced the locomotor capacity of zebrafish larvae, increased the levels of ROS and disturbed the antioxidant defense system in zebrafish larvae. In addition, a histological examination showed that the heart, liver, intestines and muscle of the $PM_{2.5}$-treated zebrafish exhibited abnormal changes and a significant increase in cellular autophagic accumulation. RT-PCR showed that the expression of genes related to inflammation (*tgfβ* and *cox2*), ERS (*hspa5*, *chop*, *ire1*, *xbp1s*, and *atf6*) and autophagy (*lc3*, *beclin1* and *atg3*) pathways was significantly increased in the $PM_{2.5}$-treated zebrafish, indicating that $PM_{2.5}$ induced inflammation and promoted ERS and autophagy responses via the activation of the IRE1-XBP1 and ATF6 pathways. Together, our data indicate that $PM_{2.5}$

* Corresponding author. Biology Institute, Qilu University of Technology (Shandong Academy of Sciences), 250103, Jinan, Shandong Province, China.
** Corresponding author.
E-mail addresses: xiaohan_0818@163.com (Y. Zhang), hliukch@sdas.org (K. Liu).

https://doi.org/10.1016/j.chemosphere.2018.01.092

induced a dose- and time-dependent increase in developmental toxicity to zebrafish embryos. Additionally, ERS and autophagy may play important roles in $PM_{2.5}$-induced developmental toxicity.

1. Introduction

Air pollution is a major environmental health threat worldwide, especially in developing countries. Fine particulate matter ($PM_{2.5}$) represents a significant air pollutant and is defined as a mixture of inorganic ions, metals, polycyclic aromatic hydrocarbons, and other particles that are 2.5 μm or less in diameter (Cheng et al., 2017). Because of its small size, $PM_{2.5}$ can penetrate deep into the alveoli of lungs and potentially into the blood circulation across the air-blood barrier, and it can even reach other organs (Duan et al., 2017a). Recently, toxicological studies confirmed that $PM_{2.5}$ is associated with an increased risk of cardiopulmonary diseases, cerebrovascular diseases and lung cancer as well as with premature birth, stillbirth and birth defects (Duan et al., 2017b; Jedrychowski et al., 2009). Although $PM_{2.5}$ has raised public concern regarding its impacts on human health, the effects of $PM_{2.5}$ on fetal growth are poorly understood. Thus, the mechanism underlying $PM_{2.5}$-induced developmental toxicity should be investigated.

Zebrafish (*Danio rerio*) is a reliable, sensitive and economic model, and it is generally used as an in vivo model to assess the toxicity of various chemicals (Dumitrescu et al., 2017). This animal is easy to handle and has a small size, high fecundity, visible embryological phases, and undergoes rapid embryogenesis and organogenesis in vitro (McGrath and Li, 2008). There is extensive synteny between zebrafish and human genomes, and zebrafish genes share a 60–80% homology with their human counterparts (Barbazuk et al., 2000). In addition, the amino acid sequences of functionally relevant protein domains in zebrafish has been proven to be even more evolutionary conserved (Reimers et al., 2004; Renier et al., 2007). And zebrafish also exhibits similarities at the physiological and molecular levels with humans in the cardiovascular system, respiratory system, immune system and other aspects (Liu et al., 2017; Muller et al., 2016; Rahbar et al., 2016). Moreover, good correlations with mammalian toxicity has been observed (Lantz-McPeak et al., 2015); therefore, zebrafish has been used as a universal model to investigate the toxicity and mechanisms of action during the early stages of embryonic development (Zou et al., 2017).

Kim et al. found water extract of PM2.5 induced oxidative stress as a precursor to cardiovascular toxicity, skin cell senescence, and embryonic toxicity via aggregation and proteolytic degradation of serum lipoproteins (Kim et al., 2015). A recent investigation showed that PM2.5 induced the cardiovascular toxicity, hepatotoxicity and neurotoxicity in zebrafish, suggested that PM2.5 could cause multi-organ toxicity in aquatic organism (Duan et al., 2017a,b). However, the cellular effects of PM2.5 and its mechanism of developmental toxicity remain poorly understood.

Previously available data have confirmed that PM2.5 could release inflammatory cytokines and activate ROS, and are also associated with cell death and genetic toxicity (Jia et al., 2017). Inflammation is an adaptive response of the body to ensure removal of harmful stimuli, as well as a healing process for repairing damaged tissue. However, sustained or chronic inflammation is detrimental (Medzhitov, 2008). Intriguingly, there is a growing evidence that inflammation is both a cause and consequence of endoplasmic reticulum stress (ERS) (Bettigole et al., 2015). Severe ERS and increasing amounts of ROS may activate signaling pathways that lead to autophagic cell death, and the integration of these responses is critical to the pathogenesis of a variety of diseases (Song et al., 2017). These findings suggest that the toxic reactions caused by PM2.5 may be associated with inflammation and the promotion of ERS and autophagy. Nonetheless, the detailed molecular mechanism underlying this process is still unclear. Therefore, in the present study, we investigated the adverse effects of PM2.5 exposure on the malformation, locomotor capacity, oxidative stress and inflammatory response of zebrafish embryos. To investigate the mechanism underlying the developmental toxicity of $PM_{2.5}$, the modulation of genes involved in ERS and autophagy signaling pathways were examined.

2. Materials and methods

2.1. $PM_{2.5}$ collection and preparation

$PM_{2.5}$ was collected on glass fiber filters using a MH-1200 automatic atmospheric particulate matter sampler (Qingdao Minghua Electronic Instrument Co., Ltd., China) at the building roof (approximately 20 m above ground). The sampling site was located in the urban area of Jinan, China from November 2016 to April 2017. After sampling, the filters with $PM_{2.5}$ were cut into small pieces and then sonicated in ultrapure water for 60 min using a KQ2200DV water-bath sonicator (Kunshan Ultrasonic Instruments, China). The obtained $PM_{2.5}$ suspension was concentrated using a vacuum-freeze dry method, and the final $PM_{2.5}$ samples were pooled together and stored at −20 °C. The major chemical components of $PM_{2.5}$ included organic carbon and elemental carbon (OC and EC), polycyclic aromatic hydrocarbons (PAHs), inorganic elements and water soluble inorganic ions. The contents of NO_3^-, SO_4^{2-}, NH_4^+ and Cl^- in PM2.5 were 142,038.9 mg/kg, 127,348.7 mg/kg, 89,536.7 mg/kg and 61,732.8 mg/kg, respectively. In metal analysis for PM2.5, the contents of aluminum, lead and manganese were 2568.4 mg/kg, 678.9 mg/kg and 445.8 mg/kg, respectively. In PAHs analysis for PM2.5, the contents of acenaphthylene, acenaphthene and two hydrogen naphthalene were 1168.0 mg/kg, 281.7 mg/kg and 160.8 mg/kg, respectively. Concentrated $PM_{2.5}$ was dissolved in the fish-tank water (5 mM NaCl, 0.17 mM KCl, 0.4 mM $CaCl_2$, 0.16 mM $MgSO_4$) according to the experimental concentrations before the experiments.

2.2. Zebrafish maintenance and exposure

Wild-type zebrafish (AB strain) and transgenic zebrafish (Tg:zlyz-enhanced green fluorescent protein (EGFP)) were obtained from the Zebrafish Drug Screening Platform of the Shandong Academy of Sciences (Jinan, China). Zebrafish embryos were maintained and raised according to the protocol described by Westerfield et al. (1992). Zebrafish were kept at 28 ± 0.5 °C under a 14:10 h light:dark cycle in a closed flow-through system with charcoal-filtered tap water. The zebrafish embryos were obtained from spawning adult male and female zebrafish at a 2:1 ratio in a translucent plastic tank within 30 min after the onset of light in the morning. Healthy embryos at 4 h post-fertilization (hpf) were distributed into six-well cell culture plates (10 embryos/well) and exposed to $PM_{2.5}$ at the doses of 200, 300, 400, 500, 600 and

800 μg/mL for a period of 120 h at 28 °C. Zebrafish treated with fish water were used as the vehicle control. The solutions were replaced and dead embryos were discarded every 24 h. Treatments were performed in three parallel replicates, and experiments were carried out in compliance with the standard ethical guidelines. During 120 hpf, the embryos were examined under a stereomicroscope (Olympus SZX16; Tokyo, Japan) to observe morphological abnormalities. The mortality and hatching rates were recorded within each group daily.

2.3. Morphology score and body lengths

Morphology scores were determined at 120 hpf to distinguish the severity of the developmental toxicity effects observed in multiple organ systems (body shape, face, brain, somites, notochord, swim bladder, yolk sac, tail, fins and pharyngeal arches/jaws) of the zebrafish larvae after exposure to $PM_{2.5}$. The morphological scoring criteria used in our study were previously described (Panzica-Kelly et al., 2010).

The length of each zebrafish larvae along the body axis from the anterior-most part of the head to the tip of the tail was recorded at 120 hpf using Image-Pro Plus software (Media Cybernetics, Bethesda, MD, USA).

2.4. Behavioral analysis

Eight larvae from each group were selected for the behavioral test at 120 hpf. Additionally, each larva was placed into one well of a 48-well plate. The larvae were incubated for 30 min at 28 °C. Next, we used ZebraLab software (Viewpoint, France) to analyze the digital tracks for 10 min.

2.5. Leukocyte migration

The transgenic zebrafish (Tg:zlyz-EGFP) that expressed EGFP in the leukocytes were used in this study. Healthy embryos at 4 hpf were distributed into six-well cell culture plates (10 embryos/well) and exposed to $PM_{2.5}$ at the doses of 200, 300, 400 μg/mL for 120 h at 28 °C. At 120 hpf, each zebrafish larva was imaged using a fluorescence microscope (Olympus, SZX16, Tokyo, Japan), and the number of leukocytes in the region of interest were recorded by Image-Pro Plus software.

2.6. Measurement of ROS generation

At 120 hpf, ROS generation in the zebrafish larvae was measured using 2′, 7′-dichlorodihydrofluorescein diacetate (DCF-DA). The larvae were incubated in a solution of 20 μg·mL-1 DCF-DA for 1 h in the dark at 28 °C. Next, the larvae were washed with fresh fish water and anesthetized with 0.16% tricaine. Finally, the larvae were imaged using a fluorescence microscope (Olympus, Tokyo, Japan), and the fluorescence intensity was quantified using the ImageJ program.

2.7. Measurement of SOD, GSH and MDA levels

At 120 hpf, 150 zebrafish larvae were homogenized in cold saline (1 g of tissue in 9 mL of normal saline). The homogenates were centrifuged at 2500 rpm at 4 °C for 10 min, and the supernatants were collected for subsequent tests. The superoxide dismutase (SOD) activity as well as the total glutathione (GSH) and malondialdehyde (MDA) levels were determined using the kits according to the manufacturer's instructions (Nanjing Jiancheng Biotechnology Institute, China).

2.8. Histopathological and ultrastructural evaluations

To examine the histopathological changes in the main organs, the zebrafish larvae were fixed in 4% paraformaldehyde, embedded in paraffin, sectioned and then stained with hematoxylin and eosin (H and E) at 120 hpf. In addition, other zebrafish larvae were fixed in glutaraldehyde paraformaldehyde solution for 24 h for electron microscopic examinations.

2.9. Total RNA extraction and RT-PCR

Total RNA was extracted from zebrafish larvae tissue using the NanoMag Animal and Fish RNA Isolation Kit (Shannuo Scientific Company, China). One microgram of total RNA was subjected to cDNA synthesis using PrimeScript@ RT Master Mix. Real-time PCR was performed in a total volume of 20 μl containing 10 μl of SYBR Green supermix, 1 μl of cDNA, 7 μl of RNase/DNase-free water and 500 nM of each primer. Gene expression was analyzed using the $2^{-\Delta\Delta CT}$ method, and *β-actin* was used as a reference gene. The sequences of primers for real-time PCR are shown in Supplementary Table 1.

2.10. Statistical analyses

Data were presented as the mean ± standard error (SE). Significant differences between groups were determined using one-way analysis of variance (ANOVA) and Dunnett's *t*-test. Statistical differences were considered significant at * $P < 0.05$ or ** <0.01.

3. Results

3.1. Mortality in PM2.5-exposed zebrafish

The mortality rates of zebrafish embryos exposed to different concentrations of $PM_{2.5}$ for 24–120 hpf are shown in Fig. 1A. Doses lower than 200 μg/mL showed no significant difference in the mortality from 24 hpf to 120 hpf. However, all fish died at exposure concentrations of 800 μg/mL and 600 μg/mL at 72 hpf and 96 hpf, respectively. Compared with control larvae, the larvae exposed to 400 and 500 μg/mL $PM_{2.5}$ showed a sharp increase in mortality at 120 hpf.

3.2. Hatching rate in PM2.5-exposed zebrafish

The hatching rates are shown in Fig. 1B. Significantly decreased hatching rates were observed at 48 hpf and 72 hpf for concentrations higher than 300 μg/mL and 500 μg/mL, respectively. Furthermore, only sporadic embryo hatching was observed in the group incubated with 800 μg/mL of $PM_{2.5}$ by 72 hpf. These data indicated a remarkable dose-dependent decrease in the hatching rate induced by $PM_{2.5}$ (Fig. 1B).

3.3. Malformations in PM2.5-exposed zebrafish

The phenotypic defects caused by $PM_{2.5}$ from 24 hpf to 120 hpf are shown in Figs. 1C and 2A. An apparent delay in hatching was found at high doses of $PM_{2.5}$. In the 200 μg/mL PM2.5 group, there was no malformation observed. In the 300 μg/mL PM2.5 group, malformation became apparent, including absence of swimming bladder, slightly yolk retention and pericardial edema. When PM2.5 concentration increased to 400 μg/mL, developmental abnormalities became more severe including severely yolk retention, swimming bladder absence, curved body shape, tail bending, pericardial edema, face and eye defects, were induced by $PM_{2.5}$. These growth defects may be caused by abnormal cell death.

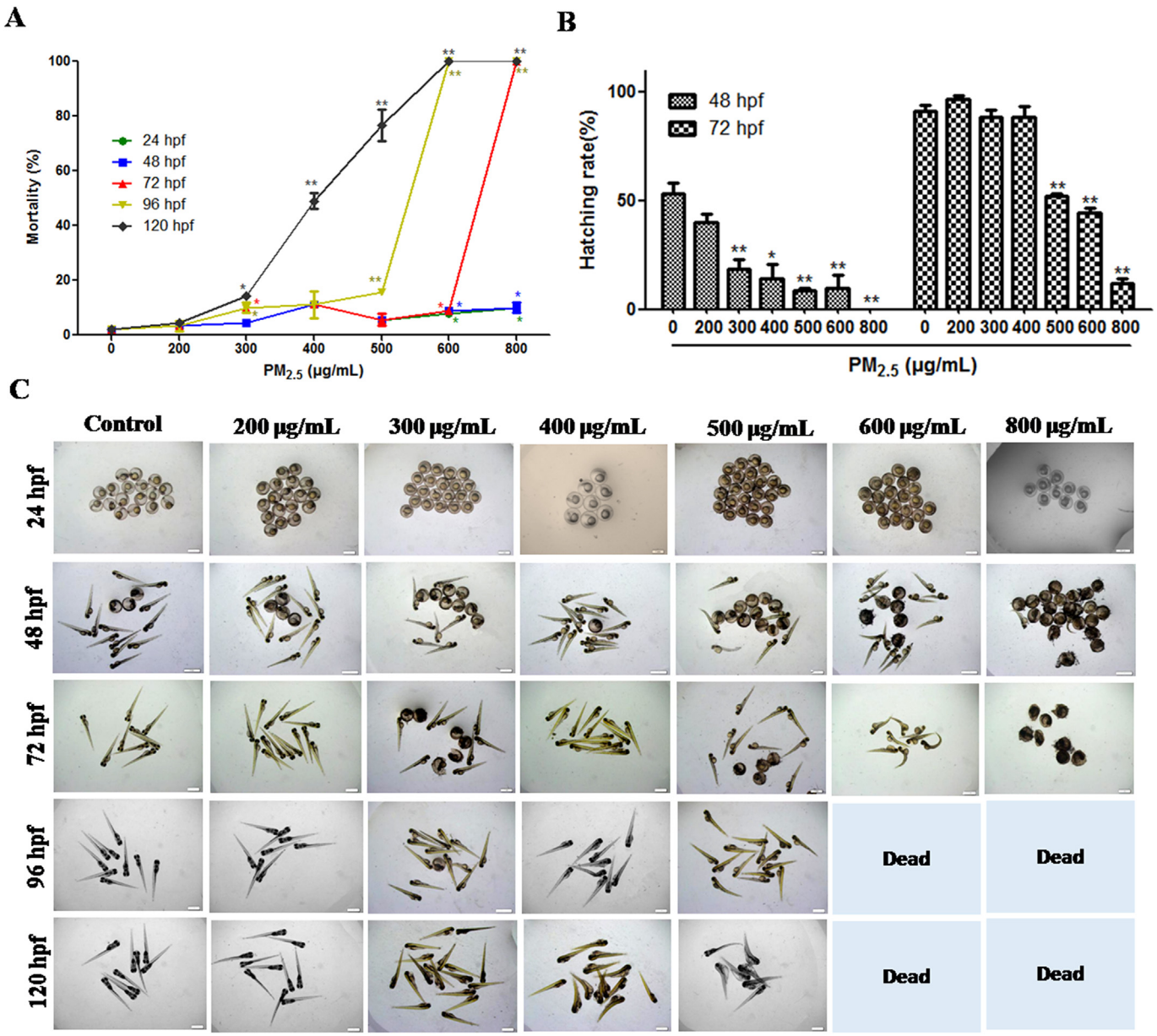

Fig. 1. Developmental toxicity effect of $PM_{2.5}$ in zebrafish embryos. (A) Mortality rate in zebrafish embryos exposed to $PM_{2.5}$ from 24 to 120 hpf. (B) Hatching rate in zebrafish embryos exposed to $PM_{2.5}$ at 48 and 72 hpf. (C) Phenotypes of zebrafish embryos exposed to $PM_{2.5}$ from 24 to 120 hpf. $^{*}P < 0.05$, $^{**}P < 0.01$ versus control.

The general morphological scoring of $PM_{2.5}$-exposed zebrafish larvae at 120 hpf is shown in Fig. 2B. The general morphological scoring criteria were described in the previous literature (Panzica-Kelly et al., 2010). Our results showed that the morphology score decreases as the $PM_{2.5}$ exposure concentration increases.

3.4. Body length in PM2.5-exposed zebrafish

Changes in the body lengths of the larvae were used as an indicator to assess the degree of development. The body lengths of the larvae were significantly decreased in the $PM_{2.5}$-treated groups compared with those in the control group (Fig. 2C). Our results showed that $PM_{2.5}$ significantly inhibited larval growth in a dose-dependent manner.

3.5. Locomotor capacity in PM2.5-exposed zebrafish

Behavioral tests were performed on larvae at 120 hpf. The digital tracks are shown in Fig. 3A. In the digital tracks map, fast movement, medium movement and slow movement are indicated by red lines, green lines and black lines, respectively. Compared with control larvae, the larvae exposed to 300 and 400 μg/mL $PM_{2.5}$ showed remarkable decreases in the total movement distance and average speed (Fig. 3B and C). These results indicated that exposure to $PM_{2.5}$ at high doses resulted in a reduction in the locomotor capacity of zebrafish larvae.

3.6. Leukocyte migration in PM2.5-exposed zebrafish

We studied the effect of $PM_{2.5}$ on leukocyte migration during the induction phase of inflammation using transgenic zebrafish

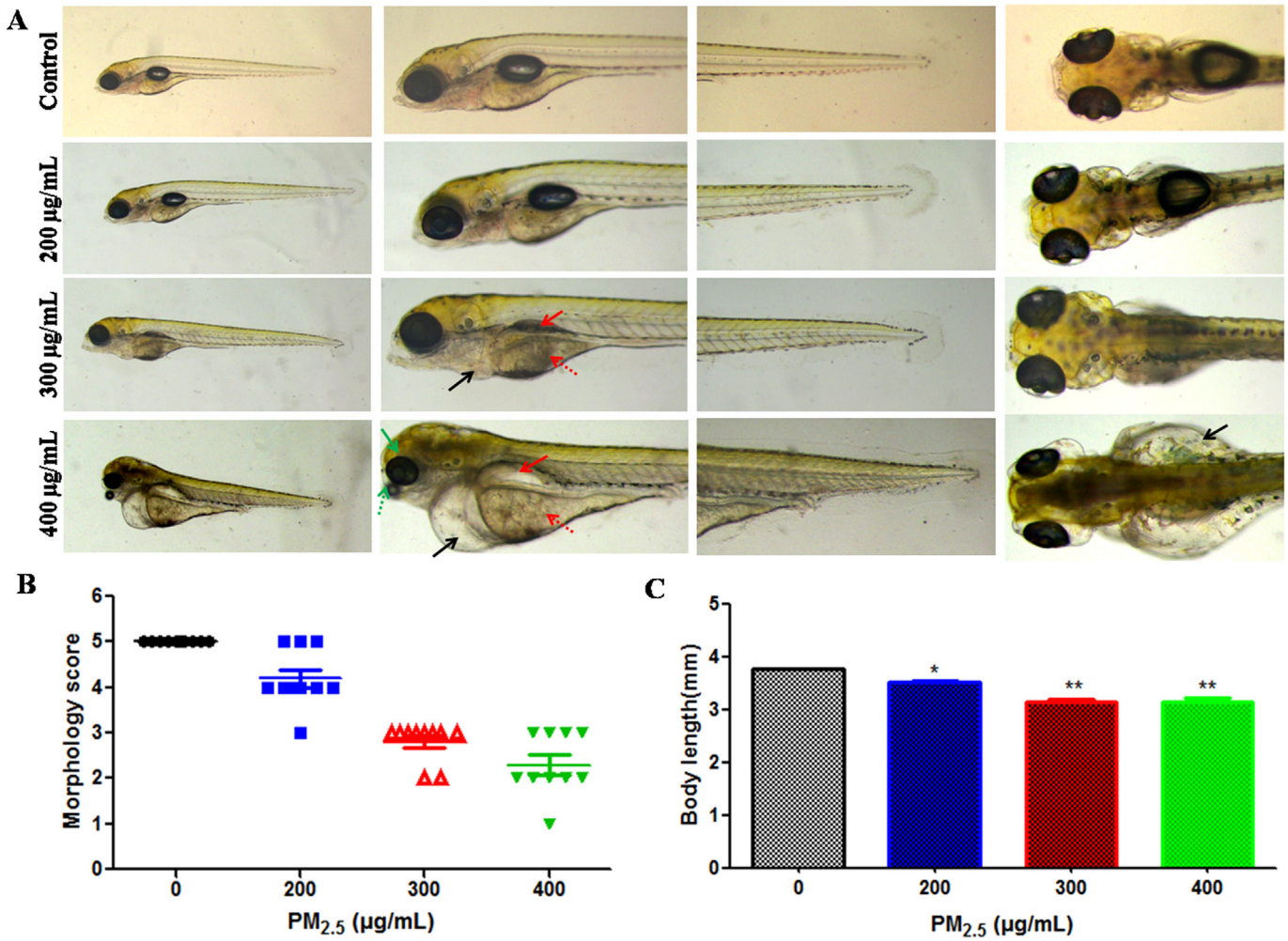

Fig. 2. Effects of $PM_{2.5}$ on morphological changes in zebrafish larvae at 120 hpf. (A) Representative lateral and ventral views, (B) morphological scoring and (C) body length of zebrafish larvae treated with $PM_{2.5}$ at 0, 200, 300 and 400 μg/mL. The absence of a swim bladder is indicated by red solid arrowheads; yolk retention is indicated by red dotted arrowheads; pericardial edema is indicated black solid arrowheads; eye defects are indicated by green solid arrowheads; and face defects are indicated by green dotted arrowheads. $^{*}P < 0.05$, $^{**}P < 0.01$ versus control. (For interpretation of the references to colour in this figure legend, the reader is referred to the Web version of this article.)

(Tg:zlyz-EGFP) embryos. Monocytes/macrophages and neutrophils, which are referred to as 'leukocytes', play an important role in acute inflammation and are labeled with green fluorescent protein in Tg:zlyz-EGFP embryos. By analyzing the number of leukocytes in the region of interest (white boxes) in Fig. 4A, we found that the number of leukocytes was significantly increased in 300 and 400 μg/mL $PM_{2.5}$-treated group compared with that in the control group (Fig. 4B). Moreover, we found that $PM_{2.5}$ exposure significantly induced the leukocyte growth-induced inflammation in zebrafish larvae.

3.7. ROS measurement in PM2.5-exposed zebrafish

As shown in Fig. 4C and D, a dose-dependent increase in the generation of ROS was observed in the zebrafish larvae treated with $PM_{2.5}$. A statistically significant increase occurred at $PM_{2.5}$ doses of 300 and 400 μg/mL compared with the control, although apparent changes were not observed in the larvae treated with 200 μg/mL $PM_{2.5}$.

3.8. PM2.5 disturbed the antioxidant defense system in zebrafish

Supplementary Table 2 shows the $PM_{2.5}$ effect on the SOD, GSH and MDA levels in zebrafish larvae. MDA levels were significantly increased in the 300 and 400 μg/mL $PM_{2.5}$-treated groups, whereas the SOD activity and GSH level were significantly decreased. No apparent changes were observed in the 200 μg/mL $PM_{2.5}$-treated group.

3.9. Histopathological changes in PM2.5-exposed zebrafish

A histological examination showed that compared with the control group, the $PM_{2.5}$-treated group exhibited abnormal changes in the heart, liver, intestines and muscle. Decreased myocardial layers and cells in the heart, loose cell-to-cell contacts in the liver, frayed gut villi and thinner intestinal walls in the intestine, and sparse myofilament fibers in the muscles were observed in the larvae exposed to 300 and 400 μg/mL $PM_{2.5}$ (Fig. 5).

3.10. Electron microscopic analysis in PM2.5-exposed zebrafish

Fig. 6 illustrates the electron microscopy analysis of hepatocytes on zebrafish after exposure to $PM_{2.5}$ at 120 hpf. The results showed that the structure of the liver membrane and organelles of the zebrafish in the control group was intact. No other lesions were observed in the hepatocytes of zebrafish in the $PM_{2.5}$ (200 μg/mL)

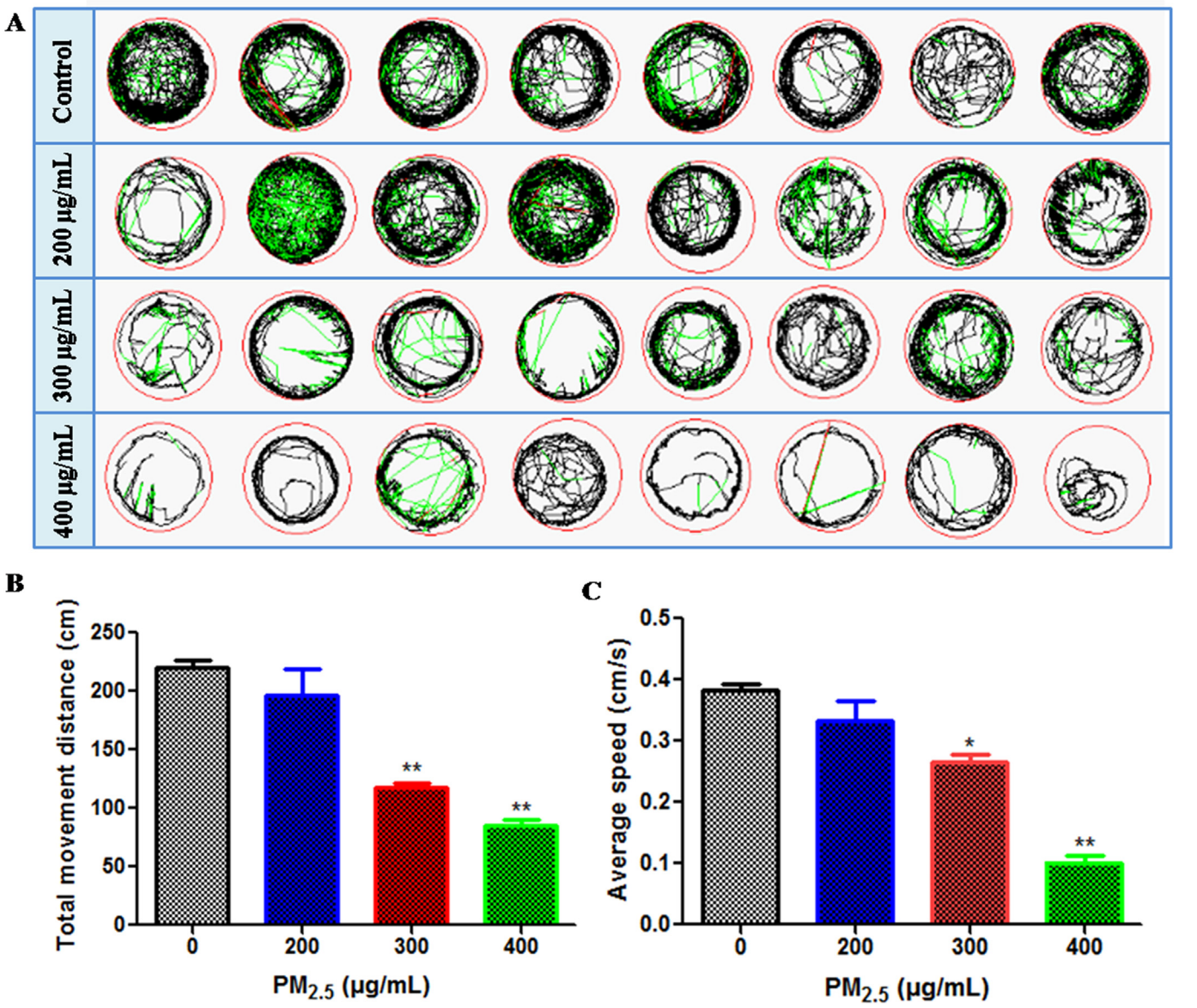

Fig. 3. Reduction of locomotor capacity of larvae exposed to $PM_{2.5}$. (A) Digital tracks, (B) total movement distance and (C) average speed of larvae in zebrafish larvae following exposure to 200, 300 and 400 μg/mL $PM_{2.5}$ at 120 hpf. $^{*}P < 0.05$, $^{**}P < 0.01$ versus control. Abbreviations: s, second.

group except for the swelling of cristae in the mitochondria of individual zebrafish. Zebrafish treated with $PM_{2.5}$ (300 and 400 μg/mL) showed significant structural abnormalities in hepatocytes. For example, the liver cell organelles dissolved, vacuoles appeared in the cytoplasm, and many autophagosomes were found in the cytoplasm.

3.11. Gene expression

To investigate the potential mechanism underlying the developmental toxicity of $PM_{2.5}$ exposure, a RT-PCR assay was performed at 120 hpf. The results verified that compared with the control group, the $PM_{2.5}$-treated group showed the up-regulation of two inflammation-related genes (*tgfβ* and *cox2*), five ERS-related genes (*hspa5*, *chop*, *ire1*, *xbp1s*, and *atf6*), and three autophagy-related genes (*lc3*, *beclin1* and *atg3*) upon exposure to 300 and 400 μg/mL by 120 hpf (Fig. 7).

4. Discussion

In the present study, zebrafish was used as an in vivo model to assess the developmental toxicity of $PM_{2.5}$. In the present study, zebrafish was used as an in vivo model to assess the developmental toxicity of PM2.5. In a preliminary study, we found that there was no apparent toxicity to embryos after treatment with PM2.5 at concentrations of 10-fold serial dilutions from 0.2 to 200 μg/mL for 4–120 hpf, and marked developmental toxicity was observed for concentrations higher than 300 μg/mL dose groups. Exposure to PM2.5 at 400 μg/mL induced 48.9% mortality until the 120 hpf, and the surviving embryos exhibited serious side effects. The 600 and 800 μg/mL concentrations of PM2.5 induced 100% mortality at 96 hpf, and all of the 1000 μg/mL PM2.5-treated embryos died at 24 hpf. Therefore, the doses of PM2.5 in our study ranged from no effect on the development to clear the toxic effect on development. Our results demonstrated dose- and time-dependent responses of zebrafish embryos to PM2.5. $PM_{2.5}$ treatment at a dose of 200 μg/

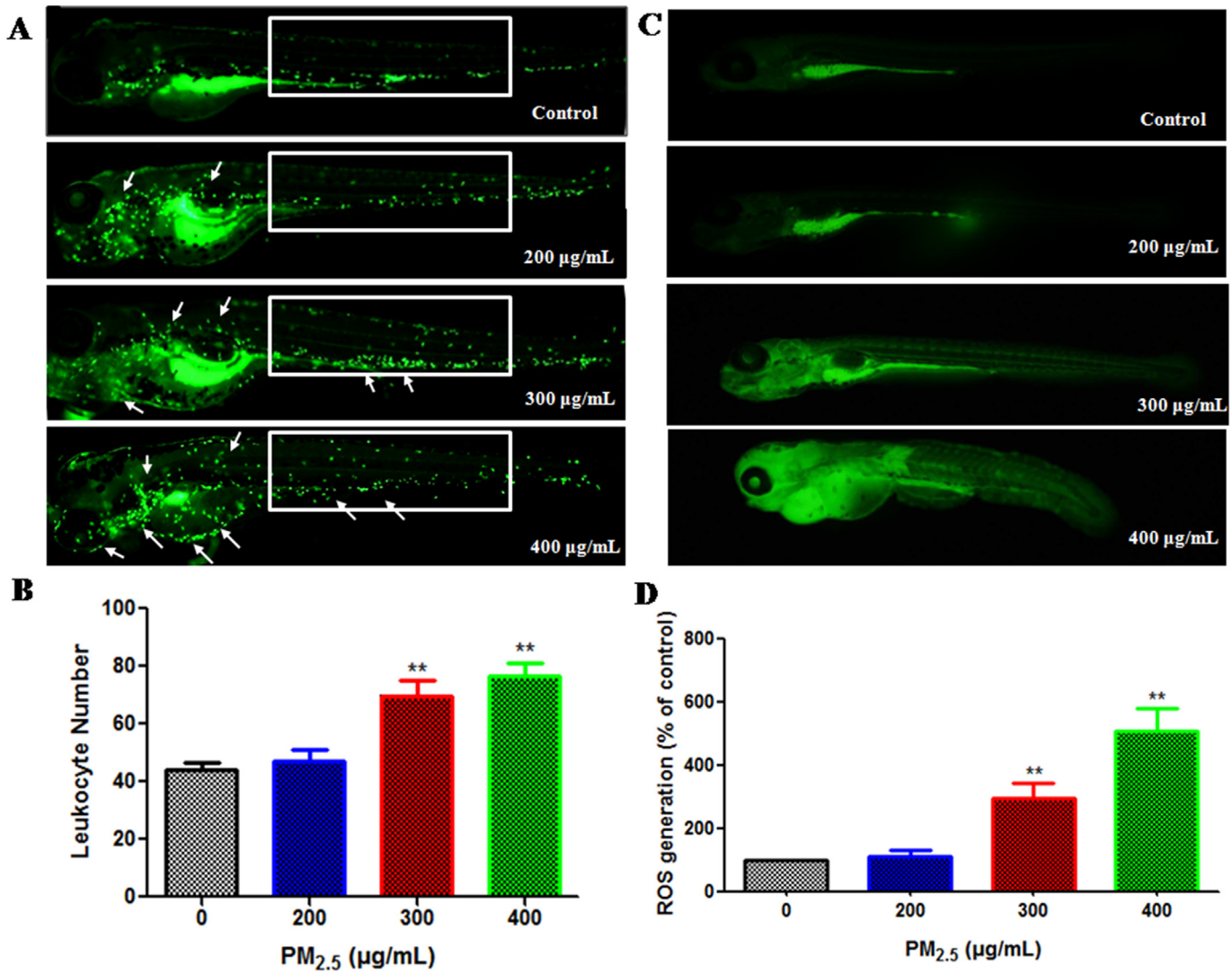

Fig. 4. Effects of $PM_{2.5}$ on leukocyte migration and ROS generation in zebrafish larvae at 120 hpf. (A) Representative images of Tg:zlyz-EGFP zebrafish exposed to $PM_{2.5}$. (B) Leukocytes in the region of interest (white boxes) were quantitatively analyzed. (C) Fluorescence micrographs of ROS generation in zebrafish larvae. (D) Quantitative analysis of ROS generation using the Image J program. $^{**}P < 0.01$ versus the control.

mL did not produce obvious signs of toxicity, whereas doses of 300 and 400 μg/mL caused significant developmental toxicity. Exposure to 300 and 400 μg/mL $PM_{2.5}$ significantly increased the mortality and malformation and reduced the hatching rate and body length of the zebrafish. The morphological abnormalities mainly included yolk retention, swimming bladder absence, curved body shape, tail bending, pericardial edema, face and eye defects. The histopathological analysis showed abnormal changes in the heart, liver, intestines and muscle in the $PM_{2.5}$-treated group compared with those in the control group. The results of this study were consistent with those of previous studies that have reported multiorgan toxicity induced by $PM_{2.5}$ (Duan et al., 2017a, 2017b).

Locomotor capacity is an indicators used to evaluate the developmental toxicology of a toxicant (Yang et al., 2011). The locomotor behavior of zebrafish occurs sequentially throughout development, including a transient period of spontaneous tail bending in the early stages of development, followed by touch-induced movement and free swimming (Brustein et al., 2003). Spontaneous movement is the first locomotor activity in the early life stage of zebrafish (Chen et al., 2017). Our results indicated that the larvae exposed to $PM_{2.5}$ (300 and 400 μg/mL) showed remarkable decreases in the total movement distance and average speed. This report is the first to demonstrate that $PM_{2.5}$ exposure can reduce locomotion ability. The present study showed that spontaneous movement in the embryo was associated with the period when primary motor neurons began to innervate muscles (Louis Saint-Amant, 1998). Previous studies have indicated that $PM_{2.5}$ could impair the nervous system and cause neuron damage in a zebrafish model (Duan et al., 2017a). In this study, the histopathological analysis showed that larvae exposed to 300 and 400 μg/mL $PM_{2.5}$ exhibited loosened and disordered arrays of muscle fibers. We speculate that $PM_{2.5}$ may disrupt motor neurons or muscle development in treated zebrafish. However, further study is still required to determine the mechanism underlying this hypothesis.

The number of leukocytes was significantly increased in the 300 and 400 μg/mL $PM_{2.5}$-treated Tg:zlyz-EGFP embryos compared with that in the control embryos, and the mRNA level of the inflammatory cytokines *tgfβ* and *cox2* were up-regulated in the $PM_{2.5}$-treated embryos. These data suggest that $PM_{2.5}$ exposure significantly induce inflammation in zebrafish larvae. Moreover, a dose-dependent increase in the generation of ROS and disruption of

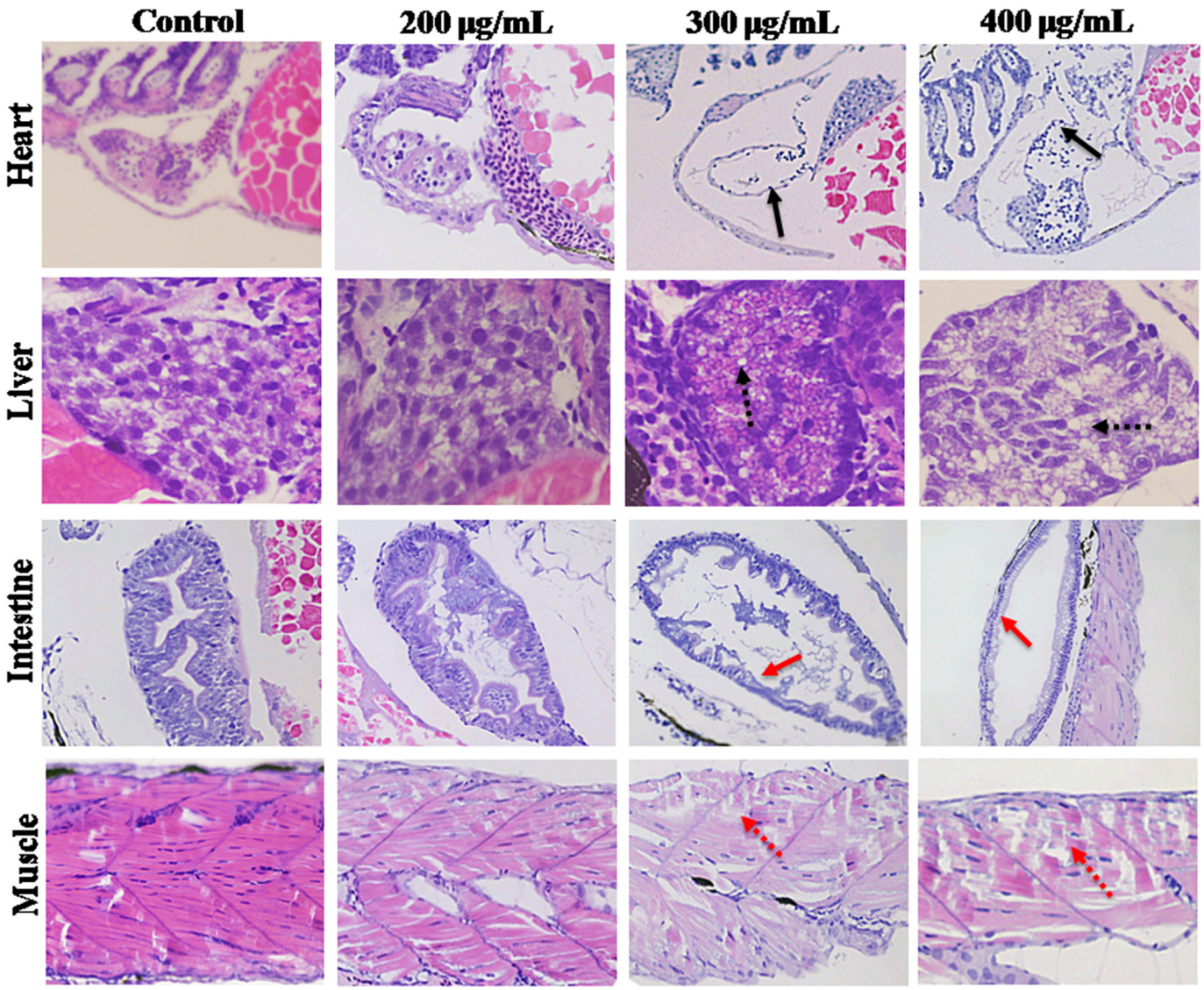

Fig. 5. Heart, liver, intestine and muscle histopathology of zebrafish after exposure to $PM_{2.5}$ at 120 hpf. Decreased myocardial layers and cells in the heart are indicated by solid black arrowheads. Loose cell-to-cell contacts in the liver are indicated by dotted black arrowheads. Frayed gut villi and thinner intestinal walls in the intestine are indicated by solid red arrowheads. Sparse myofilament fibers in the muscles are indicated by dotted red arrowheads. (For interpretation of the references to colour in this figure legend, the reader is referred to the Web version of this article.)

the antioxidant defense system (MDA increased, SOD and GSH decreased) was observed in the zebrafish larvae treated with $PM_{2.5}$. The overexpression of proinflammatory factors as well as the persistence of large amounts of ROS can cause damage to the ER or other organelles (Zeeshan et al., 2016).

To further understand the mechanism of $PM_{2.5}$-induced developmental toxicity, we analyzed the gene expression changes in the zebrafish exposed to $PM_{2.5}$ at 120 hpf. The results demonstrated that $PM_{2.5}$ affected the expression of genes involved in the ERS and autophagy pathways.

The ER is an intracellular organelle responsible for the quality control of biologically active proteins, such as synthesis, folding, posttranslational modification, and delivery (Yang et al., 2015). The accumulation of unfolded proteins could induce an adaptive program called the unfolded protein response (UPR), which is an ERS pathway (Fu et al., 2016). The primary purpose of the UPR is to facilitate the adaptation of cells to environmental changes and reestablish normal ER functions; however, the UPR also results in cell death when ER stress is severe and prolonged (Rubiolo et al., 2014). The UPR is activated by three signaling pathways—the protein kinase RNA-activated-like ER kinase (PERK)-eukaryotic translation initiation factor 2 alpha (eIF2α) pathway, the inositol-requiring enzyme 1 (IRE1)-X-box binding protein 1 (XBP1) pathway, and the activating transcription factor 6 (ATF6) pathway (Komoike and Matsuoka, 2013). GRP78 (gene name of zebrafish is *hspa5*) is an ER-resident chaperone and a central regulator of ER homeostasis that activates UPR signaling when unfolded or misfolded proteins accumulate in the ER (Walter, 2011). IRE1 is the most conserved ER stress sensor (Cao and Kaufman, 2014). IRE1α phosphorylation triggers a conformational shift that activates its C-terminal endoribonuclease activity. The endoribonuclease then excises 26 base pairs from the XBP1 mRNA, and subsequent mRNA relegation causes a translational reading frame shift yielding the highly active transcription factor known as spliced X-box binding protein 1 (XBP1S) (Calfon et al., 2002; Yoshida et al., 2001). The mRNA expression of *xbp1s* was analyzed by PCR to monitor ER

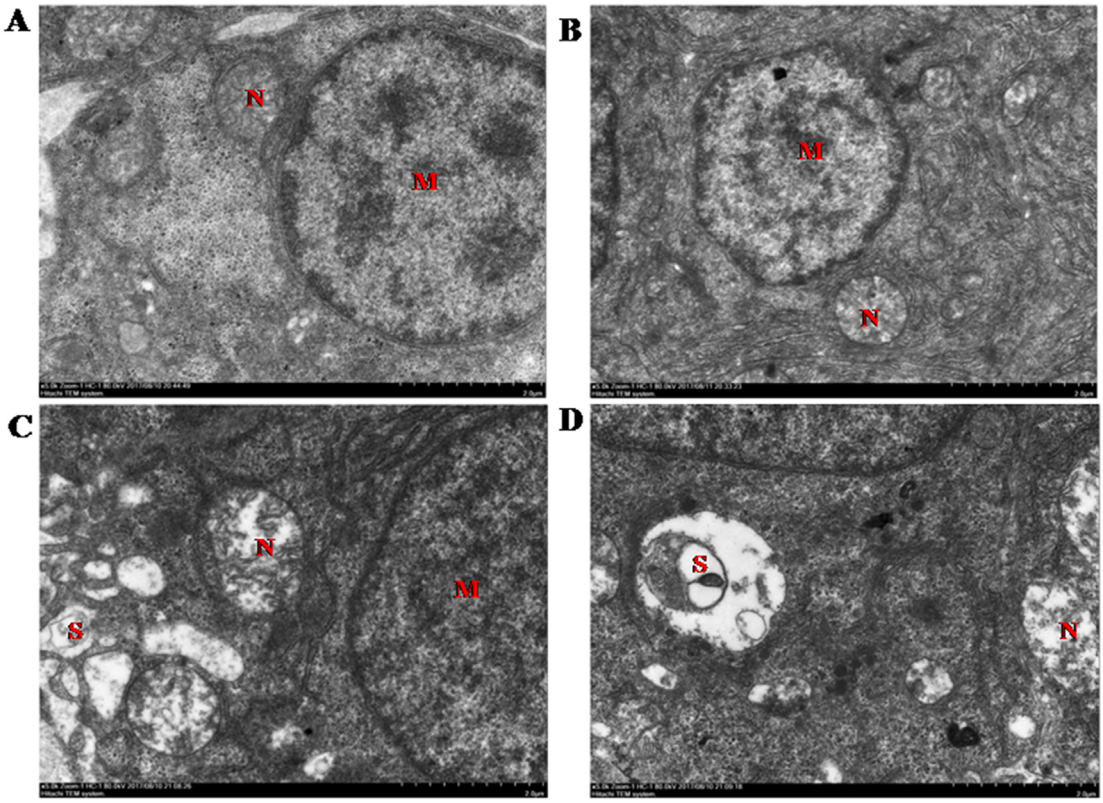

Fig. 6. Electron microscopy results of zebrafish after exposure to $PM_{2.5}$ at 120 hpf (TEM 5000×). (A) Hepatocytes in the control group. (B) Hepatocytes in the $PM_{2.5}$ (200 μg/mL) group. (C) Hepatocytes in the $PM_{2.5}$ (300 μg/mL) group. (D) Hepatocytes in the $PM_{2.5}$ (400 μg/mL) group. Nucleus (N), mitochondria (M), and autophagosome (S).

stress in our study. Additionally, CHOP is an ERS-related apoptosis factor and a downstream target gene of the UPR pathways (Shimodaira et al., 2014). In the present study, we found that $PM_{2.5}$ increased the levels of *hspa5*, *chop*, *ire1*, *xbp1s*, and *atf6* mRNA, indicating that $PM_{2.5}$ induced ERS in zebrafish via the IRE1-XBP1 and ATF6 pathways.

Simultaneously, our results showed that $PM_{2.5}$ also increased the expression level of autophagy genes, such as *lc3*, *beclin1* and *atg3*. Ultrastructural observations showed a significant increase in cellular autophagic accumulation. Autophagy is a multistep biological process. Upstream factors, such as Beclin1, FIP200 and Ambra1, are involved in the initiation and nucleation of autophagy, and downstream factors, such as Atg3, Atg5, Atg7 and LC3, promote the extension and closure of the autophagic membrane (Song et al., 2017). Although most studies have indicated that autophagy is activated for cell survival after ERS, excessive activation of autophagy induced by the heightened duration/degree of ERS can lead to cell damage (Rubiolo et al., 2014). Some have shown that ER stress can activate the autophagy mediated by PERK and IRE1 signaling (Feng et al., 2017). XBP1 is a transcription factor mediated by the IRE1α RNAse domain and can trigger autophagy via the transcriptional activation of Beclin-1 (Margariti et al., 2013). Additionally, ATF6 was reported to indirectly regulate autophagy via XBP1 and CHOP (Song et al., 2017).

Furthermore, Numerous lines of evidence have indicated that inflammation can promote ERS and autophagy. Proinflammatory cytokines, such as COX2, can inhibit the ER calcium pump and induce ER stress by up-regulating the expression of iNOS (Cardozo et al., 2005), indicating that PM2.5-induced inflammation could trigger ER stress. This ER calcium leak can then directly drive mitochondrial ROS production, affecting downstream signaling pathways and sensitizing cells to autophagy (Song et al., 2017). Autophagy is activated soon after birth in neonatal tissues and is essential for development and survival. Autophagy plays an important role in the development of cell and tissue balance, specialization, tissue differentiation, and organogenesis (Carloni et al., 2016). However, autophagy may also promote cell death through excessive self digestion and degradation of essential cellular constituents, and induce toxicity in the development process of zebrafish embryos (Rubiolo et al., 2014; Liu and Levine, 2014). Besides, it is interesting to note that the three major UPR signaling branches that are activated by ER stress are known to stimulate the expression of inflammatory cytokines and activation of NF-κB (Hotamisligil, 2010), implying that PM2.5-elicited ER stress might be a contributing factor in inflammatory process. It is now clear that inflammation, ER stress and autophagy are tightly integrated and can influence each other (Zhang et al., 2013). In this study, we found that exposure to PM2.5 increased inflammation-associated gene levels (*tgfβ and cox2*), caused the up-regulation of ERS genes, such as *hspa5*, *chop*, *ire1*, *xbp1s*, and *atf6*, and induced levels of autophagy-associated genes (*lc3, beclin1 and atg3*). These results suggest that inflammation and ERS-induced autophagy are involved in PM2.5-induced developmental toxicity in zebrafish. Further research will be required to determine the cross-talks between these stress responses in developmental toxicity arising from PM2.5 exposure, and subsequently find out the common upstream regulators.

5. Conclusions

This study presents the developmental toxicity of $PM_{2.5}$ in zebrafish. $PM_{2.5}$ exposure caused dose- and time-dependent toxic effects on zebrafish embryos, including the suppression of embryonic development and disruption of zebrafish behavior.

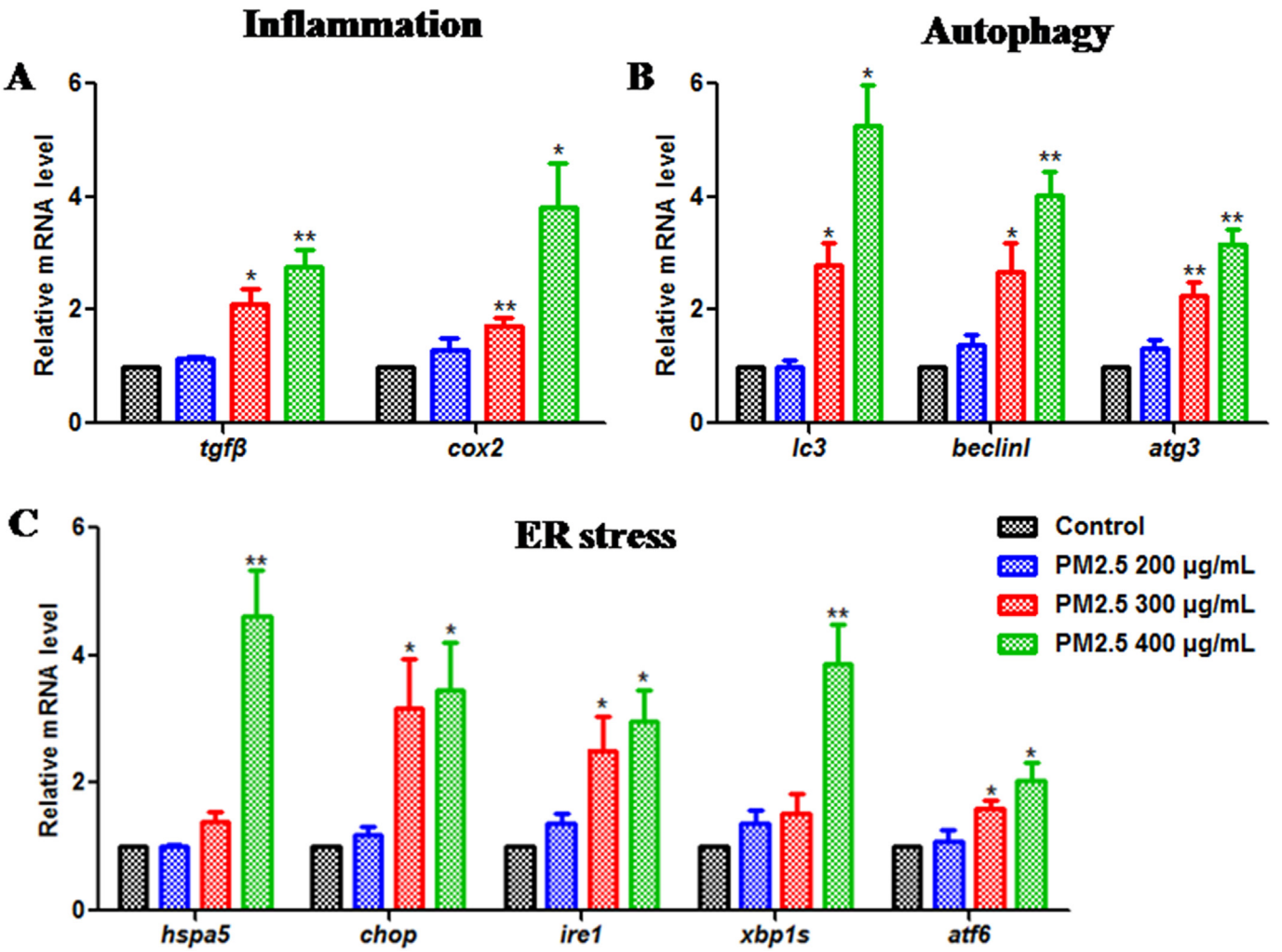

Fig. 7. Expression of inflammatory-, ER stress- and autophagy-related gene signaling pathways following $PM_{2.5}$ exposure (n = 30). $^{*}P < 0.05$, $^{**}P < 0.01$ versus control.

Additionally, $PM_{2.5}$ exposure caused increases in ROS and disrupted the antioxidant defense system. Our study revealed that exposure of zebrafish to $PM_{2.5}$ induced inflammation and promoted ERS and autophagy responses via the activation of the IRE1-XBP1 and ATF6 pathways of the UPR. Altogether, the findings reported in this study could provide insights into the mechanisms underlying $PM_{2.5}$-induced developmental toxicity.

Conflicts of interest

The authors declared no conflict of interest.

Acknowledgments

This study was supported by National Natural Science Foundation of China (No. 81703624) and Natural Science Foundation of Shandong Province (No. ZR2015YL010 and ZR2016YL009).

Appendix A. Supplementary data

Supplementary data related to this article can be found at https://doi.org/10.1016/j.chemosphere.2018.01.092.

References

Barbazuk, W.B., Korf, I., Kadavi, C., Heyen, J., Tate, S., Wun, E., Bedell, J.A., McPherson, J.D., Johnson, S.L., 2000. The syntenic relationship of the zebrafish and human genomes. Genome Res. 10, 1351–1358.

Bettigole, S.E., Glimcher, Laurie H., 2015. Endoplasmic reticulum stress in immunity. Annu. Rev. Immunol. 33, 107–138.

Brustein, E., Saint-Amant, L., Buss, R.R., Chong, M., McDearmid, J.R., Drapeau, P., 2003. Steps during the development of the zebrafish locomotor network. J. Physiol. Paris 97, 77–86.

Calfon, M., Zeng, H., Urano, F., Till, J.H., Hubbard, S.R., Harding, H.P., Clark, S.G., Ron, D., 2002. IRE1 couples endoplasmic reticulum load to secretory capacity by processing the XBP-1 mRNA. Nature 415, 92–96.

Cao, S.S., Kaufman, R.J., 2014. Endoplasmic reticulum stress and oxidative stress in cell fate decision and human disease. Antioxidants Redox Signal. 21, 396–413.

Cardozo, A.K., Ortis, F., Storling, J., Feng, Y.M., Rasschaert, J., Tonnesen, M., Van Eylen, F., Mandrup-Poulsen, T., Herchuelz, A., Eizirik, D.L., 2005. Cytokines downregulate the sarcoendoplasmic reticulum pump Ca2+ ATPase 2b and deplete endoplasmic reticulum Ca2+, leading to induction of endoplasmic reticulum stress in pancreatic beta-cells. Diabetes 54, 452–461.

Carloni, S., Favrais, G., Saliba, E., Albertini, M.C., Chalon, S., Longini, M., Gressens, P., Buonocore, G., Balduini, W., 2016. Melatonin modulates neonatal brain inflammation through endoplasmic reticulum stess, autophagy, and miR-34a/silent information regulator 1 pathway. J. Pineal Res. 61, 370–380.

Cheng, L., Lau, W.K.W., Fung, T.K.H., Lau, B.W.M., Chau, B.K.H., Liang, Y., Wang, Z., So, K.F., Wang, T., Chan, C.C.H., Lee, T.M.C., 2017. PM2.5 exposure suppresses dendritic maturation in subgranular zone in aged rats. Neurotox. Res. 32, 50–57.

Chen, X., Dong, Q., Chen, Y., Zhang, Z., Huang, C., Zhu, Y., Zhang, Y., 2017. Effects of Dechlorane Plus exposure on axonal growth, musculature and motor behavior in embryo-larval zebrafish. Environ. Pollut. 224, 7–15.

Duan, J., Hu, H., Zhang, Y., Feng, L., Shi, Y., Miller, M.R., Sun, Z., 2017a. Multi-organ toxicity induced by fine particulate matter PM2.5 in zebrafish (Danio rerio) model. Chemosphere 180, 24–32.
Duan, J., Yu, Y., Li, Y., Jing, L., Yang, M., Wang, J., Li, Y., Zhou, X., Miller, M.R., Sun, Z., 2017b. Comprehensive understanding of PM2.5 on gene and microRNA expression patterns in zebrafish (Danio rerio) model. Sci. Total Environ. 586, 666–674.
Dumitrescu, E., Karunaratne, D.P., Prochaska, M.K., Liu, X., Wallace, K.N., Andreescu, S., 2017. Developmental toxicity of glycine-coated silica nanoparticles in embryonic zebrafish. Environ. Pollut. 229, 439–447.
Feng, D., Wang, B., Wang, L., Abraham, N., Tao, K., Huang, L., Shi, W., Dong, Y., Qu, Y., 2017. Pre-ischemia melatonin treatment alleviated acute neuronal injury after ischemic stroke by inhibiting endoplasmic reticulum stress-dependent autophagy via PERK and IRE1 signalings. J. Pineal Res. 62.
Fu, J.B., Chen, P., Zhang, Y.M., 2016. Endoplasmic reticulum stress is involved in 2,4-dichlorophenol-induced hepatotoxicity. J. Toxicol. Sci. 41, 745–756. Original article.
Hotamisligil, G.S., 2010. Endoplasmic reticulum stress and the inflammatory basis of metabolic disease. Cell 140, 900–917.
Jedrychowski, W., Perera, F., Mrozek-Budzyn, D., Mroz, E., Flak, E., Spengler, J.D., Edwards, S., Jacek, R., Kaim, I., Skolicki, Z., 2009. Gender differences in fetal growth of newborns exposed prenatally to airborne fine particulate matter. Environ. Res. 109, 447–456.
Jia, Y.Y., Wang, Q., Liu, T., 2017. Toxicity research of PM2.5 compositions in vitro. Int. J. Environ. Res. 14, 232–241.
Kim, J.Y., Lee, E.Y., Choi, I., Kim, J., Cho, K.H., 2015. Effects of the particulate Matter2.5 (PM2.5) on lipoprotein metabolism, uptake and degradation, and embryo toxicity. Mol. Cell. 26, 1096–1104.
Komoike, Y., Matsuoka, M., 2013. Exposure to tributyltin induces endoplasmic reticulum stress and the unfolded protein response in zebrafish. Aquat. Toxicol. 142–143, 221–229.
Lantz-McPeak, S., Guo, X., Cuevas, E., Dumas, M., Newport, G.D., Ali, S.F., Paule, M.G., Kanungo, J., 2015. Developmental toxicity assay using high content screening of zebrafish embryos. J. Appl. Toxicol. 35, 261–272.
Liu, H., Chu, T., Chen, L., Gui, W., Zhu, G., 2017. In vivo cardiovascular toxicity induced by acetochlor in zebrafish larvae. Chemosphere 181, 600–608.
Liu, Y., Levine, B., 2014. Autosis and autophagic cell death: the dark side of autophagy. Cell Death Differ. 22, 367–376.
Louis Saint-Amant, P.D., 1998. Time course of the development of motor behaviors in the zebrafish embryo. J. Neurobiol. 37, 622–632. Saint-Amant and Drapeau.
Margariti, A., Li, H., Chen, T., Martin, D., Vizcay-Barrena, G., Alam, S., Karamariti, E., Xiao, Q., Zampetaki, A., Zhang, Z., Wang, W., Jiang, Z., Gao, C., Ma, B., Chen, Y.-G., Cockerill, G., Hu, Y., Xu, Q., Zeng, L., 2013. XBP1mRNA splicing triggers an autophagic response in endothelial cells throughBECLIN-1Transcriptional activation. J. Biol. Chem. 288, 859–872.
McGrath, P., Li, C.Q., 2008. Zebrafish: a predictive model for assessing drug-induced toxicity. Drug Discov. Today 13, 394–401.
Medzhitov, R., 2008. Origin and physiological roles of inflammation. Nature 454, 428–435.
Muller, M., Li, F., Wang, H., Liu, J., Lin, J., Zeng, A., Ai, W., Wang, X., Dahlgren, R.A., Wang, H., 2016. Immunotoxicity of β-diketone antibiotic mixtures to zebrafish (Danio rerio) by transcriptome analysis. PLoS One 11, e0152530.
Panzica-Kelly, J.M., Zhang, C.X., Danberry, T.L., Flood, A., DeLan, J.W., Brannen, K.C., Augustine-Rauch, K.A., 2010. Morphological score assignment guidelines for the dechorionated zebrafish teratogenicity assay. Birth Defects Res. Dev. Reproductive Toxicol. 89, 382–395.
Rahbar, S., Pan, W., Jonz, M.G., 2016. Purinergic and cholinergic drugs mediate hyperventilation in zebrafish: evidence from a novel chemical screen. PLoS One 11, e0154261.
Reimers, M.J., Hahn, M.E., Tanguay, R.L., 2004. Two zebrafish alcohol dehydrogenases share common ancestry with mammalian class I, II, IV, and V alcohol dehydrogenase genes but have distinct functional characteristics. J. Biol. Chem. 279, 38303–38312.
Renier, C., Faraco, J.H., Bourgin, P., Motley, T., Bonaventure, P., Rosa, F., Mignot, E., 2007. Genomic and functional conservation of sedative-hypnotic targets in the zebrafish. Pharmacogenetics Genom. 17, 237–253.
Rubiolo, J.A., Lopez-Alonso, H., Martinez, P., Millan, A., Cagide, E., Vieytes, M.R., Vega, F.V., Botana, L.M., 2014. Yessotoxin induces Er-Stress followed by autophagic cell death in glioma cells mediated by mTOR and BNIP3. Cell. Signal. 26, 419–432.
Shimodaira, Y., Takahashi, S., Kinouchi, Y., Endo, K., Shiga, H., Kakuta, Y., Kuroha, M., Shimosegawa, T., 2014. Modulation of endoplasmic reticulum (ER) stress-induced autophagy by C/EBP homologous protein (CHOP) and inositol-requiring enzyme 1alpha (IRE1alpha) in human colon cancer cells. Biochem. Biophys. Res. Commun. 445, 524–533.
Song, S., Tan, J., Miao, Y., Li, M., Zhang, Q., 2017. Crosstalk of autophagy and apoptosis: involvement of the dual role of autophagy under ER stress. J. Cell. Physiol. 232, 2977–2984.
Walter, B.M.G.a.P., 2011. Unfolded proteins are ire1-activating ligands that directly induce the unfolded protein response. Sci. Rep. 333, 1891–1895.
Westerfield, M., Wegner, J., Jegalian, B.G., DeRobertis, E.M., Puschel, A.W., 1992. Specific activation of mammalian Hox promoters in mosaic transgenic zebrafish. Genes Dev. 6, 591–598.
Yang, D., Lauridsen, H., Buels, K., Chi, L.H., La Du, J., Bruun, D.A., Olson, J.R., Tanguay, R.L., Lein, P.J., 2011. Chlorpyrifos-oxon disrupts zebrafish axonal growth and motor behavior. Toxicol. Sci. 121, 146–159.
Yang, X., Shao, H., Liu, W., Gu, W., Shu, X., Mo, Y., Chen, X., Zhang, Q., Jiang, M., 2015. Endoplasmic reticulum stress and oxidative stress are involved in ZnO nanoparticle-induced hepatotoxicity. Toxicol. Lett. 234, 40–49.
Yoshida, H., Matsui, T., Yamamoto, A., Okada, T., Mori, K., 2001. XBP1 mRNA is induced by ATF6 and spliced by IRE1 in response to ER stress to produce a highly active transcription factor. Cell 107, 881–891.
Zeeshan, H.M., Lee, G.H., Kim, H.R., Chae, H.J., 2016. Endoplasmic reticulum stress and associated ROS. Int. J. Mol. Sci. 17, 327–357.
Zhang, S., Jiang, C., Liu, H., Guan, Z., Zeng, Q., Zhang, C., Lei, R., Xia, T., Gao, H., Yang, L., Chen, Y., Wu, X., Zhang, X., Cui, Y., Yu, L., Wang, Z., Wang, A., 2013. Fluoride-elicited developmental testicular toxicity in rats: roles of endoplasmic reticulum stress and inflammatory response. Toxicol. Appl. Pharmacol. 271, 206–215.
Zou, Y., Zhang, Y., Han, L., He, Q., Hou, H., Han, J., Wang, X., Li, C., Cen, J., Liu, K., 2017. Oxidative stress-mediated developmental toxicity induced by isoniazide in zebrafish embryos and larvae. J. Appl. Toxicol. 37, 842–852.